Anisotropic electrolyte electroreflectance study of rhenium-doped MoS_2

2000 J. Phys.: Condens. Matter 12 5043

(http://iopscience.iop.org/0953-8984/12/23/312)

J. Phys.: Condens. Matter **12** (2000) 5043–5052. Printed in the UK PII: S0953-8984(00)09805-2

Anisotropic electrolyte electroreflectance study of rhenium-doped MoS_2

K K Tiong† and T S Shou

Department of Electrical Engineering, National Taiwan Ocean University, Keelung 202, Taiwan, Republic of China

E-mail: kktiong@ind.ntou.edu.tw

Received 23 November 1999, in final form 13 April 2000

Abstract. Anisotropy of rhenium-doped MoS_2 parallel and perpendicular to the c-axis ($k \parallel c$ and $k \perp c$) was studied using electrolyte electroreflectance (EER) measurements over an energy range from 1.75 eV to 4.5 eV. The measurements for $k \perp c$ were made possible by the thicker samples of MoS_2 available through introducing a small concentration of rhenium during growth. The excitonic transitions A and B for both $k \perp c$ and $k \parallel c$ configurations showed different degrees of red shift compared with that of the undoped sample. It is found that rhenium which is present as an intentionally doped impurity plays an important role in affecting the observed differences.

1. Introduction

Molybdenum disulphide belongs to the group VIA layer type transition metal dichalcogenides [1, 2], MX_2 where M = Mo, W; X = S, Se, Te. With the exception of β-$MoTe_2$ and WTe_2, which are semimetals, the rest of the families are small band gap diamagnetic semiconductors [1, 2]. The MoS_2 compound has been the subject of great interest because of the extreme anisotropic optical, electrical and mechanical properties [1–3] and their possible applications in photoelectrochemical solar cells [4–8] and as a solid lubricant [9–11]. The anisotropy of the semiconductor is a result of the sandwich interlayer structure, loosely bonded by the weak van der Waals forces [1–3, 12]. The intralayer bonding is thought to be part ionic and part covalent, with the latter being dominant [3, 12]. There are two known polytypes of MoS_2, termed 2H-MoS_2 and 3R-MoS_2 [1, 2, 13]. Both polytypes have regular layered structures with sixfold trigonal prismatic coordination of Mo atoms by the sulphur atoms within the layers. 2H-MoS_2 has two layers per unit cell stacked in hexagonal symmetry and belongs to the space group D^4_{6h} while 3R-MoS_2 has rhombohedral symmetry with three layers along the c-axis and belongs to the space group C^5_{3v}. Naturally occurring 3R-MoS_2 has been found to be consistently rich in certain minor elements such as Re, Nb etc [13]. The incorporation of the impurity elements will essentially influence the structural symmetry of MoS_2, that is the adoption of the polytype 3R-MoS_2. Early studies on the synthetic MoS_2 showed that sulphidization of pure Mo (or Mo with Re impurity) would result in 2H-MoS_2 (or 3R-MoS_2) [14]. The 3R modification of MoS_2 is a result of substitution of part of the Mo atoms by Re in the MoS_2 lattice which made the three layer 3R packing more stable than the two layer 2H polytype [14]. The influence of dopant (Re) in transforming 2H-MoS_2 to 3R-MoS_2 and

† Author to whom correspondence should be addressed.

0953-8984/00/235043+10$30.00

their anisotropic electrical properties had also been reported recently [15]. However, only few works concerning the effects of dopants in affecting the anisotropic optical properties of MoS_2 have been performed [3].

In this study, we present electrolyte electroreflectance (EER) measurements of Re-doped MoS_2 (Re–MoS_2) in the energy range 1.75 eV to 4.5 eV. The much larger surfaces available enabled both $\boldsymbol{k} \perp \boldsymbol{c}$ and $\boldsymbol{k} \parallel \boldsymbol{c}$ EER to be performed accurately. The EER technique has been proven to be a very powerful tool in the study of the band structure of semiconductors [16, 17]. The derivative nature of the EER spectrum suppresses uninteresting background effects and greatly enhances the precision in the determination of transition energies. The sharper line shapes as compared to the conventional optical measurements have enabled us to achieve a greater resolution and hence to detect weaker features. From a detailed line shape fit with a form of the Aspnes equation of the derivative Lorentzian line shape [18], the energies of the band edge excitonic transitions and higher lying interband transitions are determined accurately. The role of the rhenium impurity in influencing the change in the excitonic features will be examined. In addition, the anisotropy of $\boldsymbol{k} \perp \boldsymbol{c}$ and $\boldsymbol{k} \parallel \boldsymbol{c}$ EER spectra will also be analysed and discussed.

2. Experiment

Single crystals of the system Re–MoS_2 had been grown by the chemical vapour transport method with Br_2 as a transport agent. The total charge used in each growth experiment was about 10 g. The stoichiometrically determined weight of the doping material was added in the hope that it would be transported at a rate similar to that of Mo. Prior to the crystal growth, a quartz ampoule (22 mm OD, 17 mm ID, 20 cm length) containing Br_2 ($\sim$5 mg cm^{-3}) and the elements (Mo, 99.99% pure; Re, 99.99%; S, 99.999%) was cooled with liquid nitrogen, evacuated to 10^{-6} Torr and sealed. It was shaken well for uniform mixing of the powder. The ampoule was placed in a three zone furnace and the charge prereacted for 24 h at 800 °C with the growth zone at 950 °C, preventing the transport of the product. The temperature of the furnace was increased slowly. The slow heating was necessary to avoid any possibility of explosion due to the exothermic reaction between the elements. The furnace was then equilibrated to give a constant temperature across the reaction tube, and programmed over 24 h to produce the temperature gradient at which single-crystal growth took place. Optimal results were obtained with temperature gradient of approximately 960 $\rightarrow$ 930 °C. After 240 h, the furnace was allowed to cool down slowly (40 °C h^{-1}) to about 200 °C. The ampoule was then removed and wet tissues applied rapidly to the end away from the crystals to condense the Br_2 vapour. When the ampoule reached room temperature, it was opened and the crystals removed. The crystals were then rinsed with acetone and deionized water. Single crystalline platelets up to 10×10 mm^2 surface area and 2 mm in thickness were obtained. The as-grown rhenium-doped MoS_2 single crystal is shown in figure 1. MoS_2 crystallizes with 2H or 3R structure, while ReS_2 crystallizes in a distorted C6 structure [1], so that we do not expect the two solid solutions to be miscible. It was found that a 5% nominal doping of MoS_2 prevented the growth of single crystals [15].

The rhenium composition was estimated by energy dispersive x-ray analysis (EDX). A considerable discrepancy exists between the nominal doping ratios and those determined by EDX. The nominal concentration x is much larger than the actual one. Because no Re could be detected in EDX even though this method is sensitive for concentrations $\geqslant 1\%$, we conclude that Mo and Re metals are most likely be chemically transported at different rates and most of the doping material must remain in the 'untransported' residual charge. For the experiments, the concentration of rhenium is taken to be the nominal starting composition.

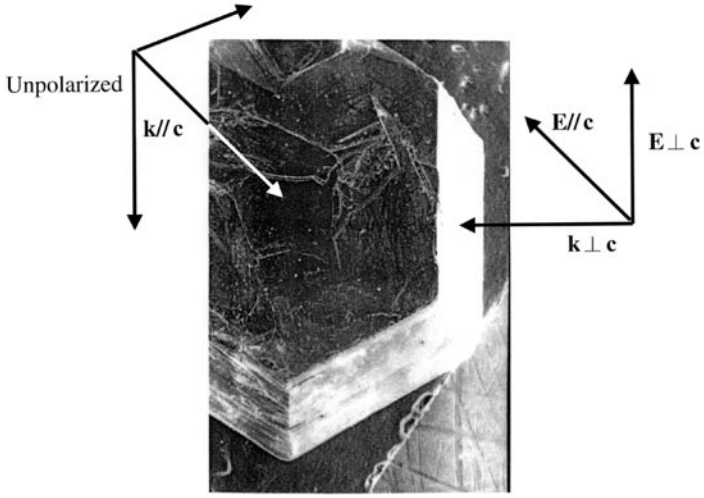

Figure 1. Photograph of the as-grown Re-doped MoS_2 showing the exposed van der Waals plane and edge plane surfaces. The experimental polarization schemes are as shown.

For the EER experiment, maximum size crystals of 1% Re-doped MoS_2 (10×10 mm^2 surface area with a thickness of 2 mm as shown in figure 1) were selected. The EER were taken on a fully computerized set-up for modulation spectroscopy described elsewhere [17–19]. The unpolarized EER spectra for Re–MoS_2 in the range 1.75 eV to 4.5 eV were recorded for reflections off the van der Waals plane surface ($\boldsymbol{k} \parallel \boldsymbol{c}$) and off the edge plane surface ($\boldsymbol{k} \perp \boldsymbol{c}$). The EER spectrum for undoped MoS_2 (2H-MoS_2) was only recorded over the same energy range for the $\boldsymbol{k} \parallel \boldsymbol{c}$ configuration since the available samples are too thin (20–100 micron thick) to allow for reliable EER measurements from the edge plane surface. A more detailed investigation of the prominent structures in the energy range 1.75–2.25 eV was also undertaken. For Re-doped MoS_2, polarized spectra with the electric field of the incident light perpendicular ($\boldsymbol{E} \perp \boldsymbol{c}$) and parallel ($\boldsymbol{E} \parallel \boldsymbol{c}$) to the $\boldsymbol{c}$-axis were recorded for $\boldsymbol{k} \perp \boldsymbol{c}$ configuration while the unpolarized spectrum was recorded for $\boldsymbol{k} \parallel \boldsymbol{c}$ configuration. For undoped MoS_2, only $\boldsymbol{k} \parallel \boldsymbol{c}$ spectrum was recorded. The polarization schemes are shown in figure 1. It is noted that for the $\boldsymbol{k} \parallel \boldsymbol{c}$ configuration, the unpolarized spectra are effectively equivalent to $\boldsymbol{E} \perp \boldsymbol{c}$ polarization. The detector response to the DC component of the reflected light is kept constant by either an electronic servo mechanism or a neutral density filter so that the AC reflectance corresponds to $\Delta R/R$, the differential reflectance. Scans of $\Delta R/R$ versus wavelength were obtained using a 0.35 m McPherson grating monochromator together with an Oriel 150 W xenon arc lamp as a monochromatic light source. Phase sensitive detection was used to measure the differential reflectance. The electrolyte was a 1 N H_2SO_4 aqueous solution, and the counter-electrode was a 5 cm^2 platinum plate. A 200 Hz 100 mV peak-to-peak square wave with $V_{DC} = 0$ V versus platinum electrode was used to modulate the electric field in the space charge region of the MoS_2 electrode.

3. Results and discussion

The unpolarized EER spectra in the energy range 1.75 eV to 4.5 eV for 1% Re-doped MoS_2 with $\boldsymbol{k} \perp \boldsymbol{c}$ (top), 1% Re-doped MoS_2 with $\boldsymbol{k} \parallel \boldsymbol{c}$ (middle) and undoped MoS_2 (bottom) are displayed in figure 2. Detailed EER spectra in the energy range 1.75 eV to 2.25 eV with various

Table 1. Energies of prominent features of undoped (or 2H-) MoS_2 and Re-doped (or 3R-) MoS_2. For exciton A, only the $n = 1$ peak is tabulated.

	Present work (energy in eV)					Work of Beal *et al* [2] (energy in eV)	
		Re-doped MoS_2					
	Undoped MoS_2		$\boldsymbol{k} \perp \boldsymbol{c}$				
	$\boldsymbol{k} \parallel \boldsymbol{c}$	$\boldsymbol{k} \parallel \boldsymbol{c}$				2H-MoS_2	3R-MoS_2
Feature	$\boldsymbol{E} \perp \boldsymbol{c}$	$\boldsymbol{E} \perp \boldsymbol{c}$	unpolarized	$\boldsymbol{E} \perp \boldsymbol{c}$	$\boldsymbol{E} \parallel \boldsymbol{c}$	$\boldsymbol{k} \parallel \boldsymbol{c}$	$\boldsymbol{k} \parallel \boldsymbol{c}$
A	1.881	1.854	1.836	1.833	1.838	1.910	1.908
B	2.070	2.005	1.984	1.984	1.984	2.112	2.057
d	2.590	2.590	—			2.63	—
C	2.800	2.764	2.764			2.760	2.758
D	2.970	2.950	2.950			3.175	3.126
	3.500	3.500	—			—	—
α	3.650	3.650	—			3.685	3.715
β	3.800	3.750	3.748			3.93	—

polarization configurations showing the most prominent excitonic features are illustrated in figure 3. The crystal symmetry of the undoped MoS_2 and Re-doped MoS_2 has been revealed by x-ray diffractometry to be hexagonal (2H) and rhombohedral (3R), respectively. In order to emphasize the role of rhenium, we choose to refer to these samples as undoped or Re–MoS_2. The experimental curves have been fitted to a Lorentzian line shape function of the form [18, 19]

$$\frac{\Delta R}{R} = \mathrm{Re} \sum_{i=1}^{m} C_i \, \mathrm{e}^{\mathrm{i}\phi_i} [E - E_i + \mathrm{j}\Gamma_i]^{-n} \tag{1}$$

where C_i and ϕ_i are the amplitude and phase of the lineshape, E_i and Γ_i are the energy and linewidth of the interband transition. For excitonic transition $n = 2$ is appropriate while $n = 2.5$ is applicable for an M_0 type critical point transition [18]. The fits yield the parameters C_i, E_i and Γ_i. The obtained values of E_i are indicated as arrows and will be used for the assignment of the transitions by comparing with the experimental results of Beal *et al* [2]. The least squares fits using equation (1) are shown as solid curves in both figures 2 and 3. The energies of the features are listed in table 1. In general, a good correspondence can be made for the recorded spectra of this work with the transmission data of Beal *et al* [2] and with the values of temperature dependent wavelength modulated reflection (WMR) spectra for excitons A and B only by Fortin and Raga [20]. However, differences do exist which can be attributed to the presence of rhenium impurity. The nomenclature A, B, AR, d, C, D, α and β adopted by previous works [1, 2] for peak assignment will also be used here. Additionally, we would like to emphasize that in this work our focus is on the role of rhenium dopant in affecting the change in the anisotropic EER spectra of the Re-doped MoS_2. In this paper, we will simply state without attempting to discuss the physical origins of the excitonic features and those of the higher lying interband transitions where relevant works can be found elsewhere [1, 2, 21–28]. From [26], the excitons A and B are being assigned to be transitions at K point, with K_1 and K_4 as the initial states, and K_5 as the final state. Feature d belongs to $\Gamma_1^+ \rightarrow \Gamma_3^+$ transition; C is assigned to be the $Q_2^- \rightarrow Q_2^-$ transition; D is a $P_3^- \rightarrow P_3^-$ transition and α and β are assigned as $\Gamma_3^+ \rightarrow \Gamma_3^+$ transitions [2]. Discussion of the experimental results will be divided into two parts: a comparative study of the excitonic and higher lying interband transitions and the role of rhenium in affecting the measured EER spectra.

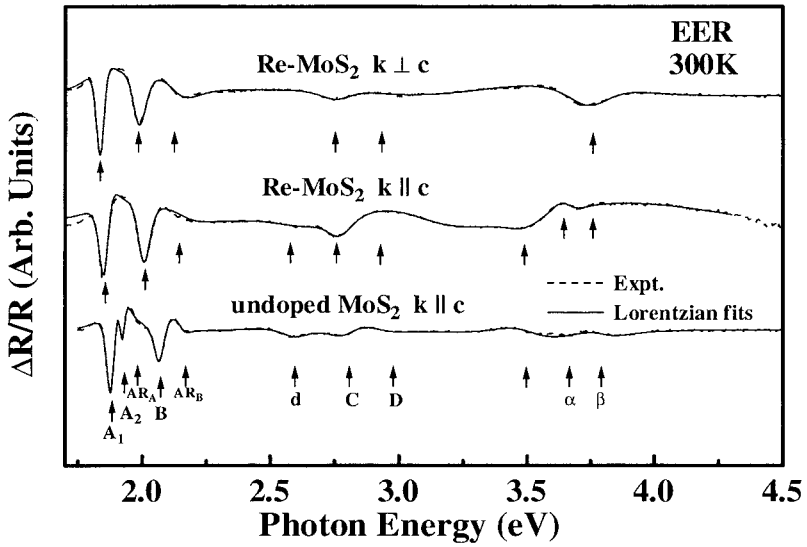

Figure 2. Unpolarized EER spectra of the Re-doped and undoped MoS_2 samples over the energy range 1.75 eV to 4.5 eV.

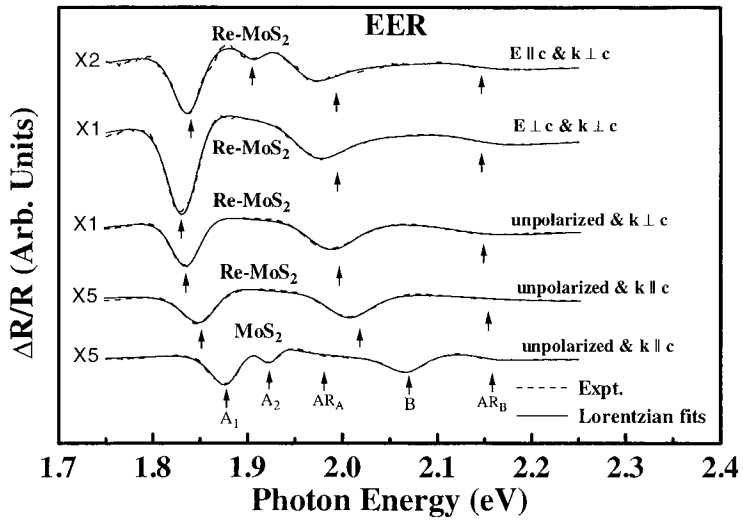

Figure 3. Polarization dependent EER spectra of Re-doped and undoped MoS_2 samples over the energy range 1.75 eV to 2.25 eV.

3.1. A comparative study of excitonic and higher lying interband transitions

The $\boldsymbol{k} \parallel \boldsymbol{c}$ EER spectrum for undoped MoS_2 is displayed at the bottom of figure 2. The energies obtained from the least squares fits are listed in table 1 together with the relevant values from the experimental work of Beal *et al* [2] for comparison purpose. In general, our room temperature results are lower than [2] where the measurements were performed at 5 K. However, the energies of excitons A and B determined in this work agreed well with that of Fortin and Raga [20] by extrapolating their data into the room temperature regime.

For exciton A, two bands (A_1 and A_2) were detected. A structure at 1.986 eV appeared as a broad shoulder on the lower energy side of exciton B was also recorded. The direct band gap and exciton binding energy for 2H-MoS_2 can be estimated by the effective mass approximation calculation, which results in a three-dimensional Mott–Wannier hydrogen-like series relation of the form [29]

$$E_n = E_g - R/n^2 \qquad n = 1, 2, 3 \ldots \tag{2}$$

where E_g and R are the band gap and exciton binding energy, respectively. From the fitted values of $E_{A_1} = 1.881$ eV and $E_{A_2} = 1.925$ eV, the direct band gap E_g is evaluated to be 1.94 eV for MoS_2 and the exciton binding energy R estimated to be 58.7 meV. These values are similar to that of Beal *et al* [2]. The broad shoulder located at 1.986 eV can be discounted as the $n = 3$ band of the exciton A series. Similar feature is also being detected by the WMR experiments of Weiser [12] and Fortin and Raga [20] and is labelled as A′ by [20]. The energy of this feature agreed well with that of [20] by extrapolating their data to room temperature. This feature is most likely the antiresonance structure (labelled as AR_A) due to the similarity of this feature to the antiresonance 'dip' structure observed at ∼2.15 eV (labelled as AR_B) [2]. The absence of $n = 2$ band for exciton B series as had been pointed out is probably due to the mixing of $n = 1$ B series with higher order states [30] forming the single detected peak at 2.07 eV. This assertion is quite reasonable considering that the linewidth of exciton B is much broader than that of exciton A.

For the Re–MoS_2 sample, the spectra of $\boldsymbol{k} \perp \boldsymbol{c}$ and $\boldsymbol{k} \parallel \boldsymbol{c}$ displayed marked differences indicating anisotropic optical properties of the doped semiconductor. Both spectra also show certain deviation as compared with the EER spectrum of undoped MoS_2. A most noticeable difference is the absence of the $n = 2$ exciton A series in the spectra of Re–MoS_2. This observation follows the general trend of transition metal dichalcogenides of 3R polytype [2]. For excitons A and B, different degrees of red shift may be obtained by comparing our results for the Re–MoS_2 sample with our undoped sample or with the transmission data of [2] on 2H- and 3R-MoS_2 samples. From Beal *et al* [2], exciton A of 2H-MoS_2 is slightly higher than that of 3R-MoS_2 while exciton B of 3R-MoS_2 is red shifted by 55 meV. In figure 2, from the spectra of undoped MoS_2 and Re–MoS_2, the red shifts of exciton A are determined to be 27 meV ($\boldsymbol{k} \parallel \boldsymbol{c}$) and 45 meV ($\boldsymbol{k} \perp \boldsymbol{c}$, unpolarized), while for exciton B the red shifts are 65 meV ($\boldsymbol{k} \parallel \boldsymbol{c}$) and 86 meV ($\boldsymbol{k} \perp \boldsymbol{c}$). The value of 65 meV for the $\boldsymbol{k} \parallel \boldsymbol{c}$ configuration is identical with the separation of the feature labelled as B* from exciton B of the WMR measurement of [20] where the same $\boldsymbol{k} \parallel \boldsymbol{c}$ configuration is being employed. The presence of B* is attributed to the coexistence of 3R and 2H phases [13, 14, 20] in their synthetic crystals. In this work, the 'purity' of the recorded spectra indicates the good quality of our samples. We also believed that the more sensitive EER technique of this work should offer better accuracy over the transmission spectra of [2]. However such a difference in measurement techniques cannot account adequately for the large variation of the excitonic transition energies between undoped and Re–MoS_2 samples. It is therefore deduced that the presence of rhenium must play an important role. A more elaborate discussion of this effect will be presented later. The location of the AR_B feature is similar for the undoped and Re-doped MoS_2 and is quite insensitive to the reflection planes. The AR_A feature is not detected in the Re–MoS_2 sample. It is most likely that the relatively weaker AR_A feature is being masked by the more dominant, red-shifted exciton B in the spectra of Re-doped MoS_2. As a result, the linewidth of exciton B for the Re–MoS_2 sample is observed to be broader than that of undoped MoS_2 whereas exciton A of the Re–MoS_2 sample appeared sharper than that of the undoped MoS_2 [2].

From this work, it is observed that the occurrences of the higher lying interband transitions are similar for both undoped and Re-doped MoS_2. The similarity is especially remarkable for

the $\boldsymbol{k} \parallel \boldsymbol{c}$ configuration. Our experimental results ($\boldsymbol{k} \parallel \boldsymbol{c}$ configuration) correspond almost in parallel to the works of Beal *et al* [2] on 2H- and 3R-MoS_2 except for some small differences. The reason is that the more sensitive EER spectra enable us to pick up much weaker features that may not be resolved in the transmission spectra of [2]. The fitted features from figure 2 are listed in table 1 for easy comparison.

3.2. Rhenium effect in the measured EER spectra

Figure 3 shows the polarized and unpolarized EER spectra of undoped and Re–MoS_2 for recorded signals reflected off the van der Waals plane and edge plane surfaces in the energy range 1.75 eV to 2.25 eV. The curve at the bottom of figure 3 is the $\boldsymbol{k} \parallel \boldsymbol{c}$, unpolarized spectrum for the undoped MoS_2 sample. The unpolarized spectrum is effectively equivalent to the $\boldsymbol{E} \perp \boldsymbol{c}$ polarization. For Re–MoS_2, the configurations are $\boldsymbol{k} \parallel \boldsymbol{c}$, unpolarized or equivalently $\boldsymbol{E} \perp \boldsymbol{c}$ polarization; $\boldsymbol{k} \perp \boldsymbol{c}$, unpolarized spectrum; $\boldsymbol{k} \perp \boldsymbol{c}$, $\boldsymbol{E} \perp \boldsymbol{c}$ and $\boldsymbol{k} \perp \boldsymbol{c}$, $\boldsymbol{E} \parallel \boldsymbol{c}$ spectra. The reason for inclusion of the $\boldsymbol{k} \perp \boldsymbol{c}$ unpolarized spectrum for the Re–MoS_2 sample will be explained. The spectrum of $\boldsymbol{k} \perp \boldsymbol{c}$, $\boldsymbol{E} \perp \boldsymbol{c}$ results in the lowest peak location for exciton A at 1.833 eV while exciton B is unaffected. The physical origin of the measured red shift of the excitonic features will be discussed. In addition to the observed red shifts of the excitonic features, extreme deviation exists between our work and that of Liang [3]. In the polarization reflectance measurements of Liang [3] on group VIA transition metal dichalcogenides with 3R phase, the exciton doublets A and B are forbidden for $\boldsymbol{k} \perp \boldsymbol{c}$, $\boldsymbol{E} \parallel \boldsymbol{c}$ polarization. A discussion of the selection rules of the excitonic features A and B can be found elsewhere [3, 26]. Our EER spectrum for the same scheme clearly shows that the selection rules for excitons A and B are not obeyed. At this point, we suspect that the rhenium impurity must have broken the selection rules somewhat such that the normally forbidden transitions become possible. This point needs further verification. The polarized spectra for Re–MoS_2 should be performed for the energy range 1.75–4.5 eV to check whether selection rules for the higher interband transitions are also compromised by the rhenium impurity. In the same $\boldsymbol{k} \perp \boldsymbol{c}$, $\boldsymbol{E} \parallel \boldsymbol{c}$ spectrum, we have also detected a clear structure located in between excitons A and B at 1.906 eV. The origin of this structure required further experimental study and is at present beyond the scope of this work.

In the following discussion, the focus is on the different physical mechanisms affecting the measured red shifts of excitons A and B. A comparison of the spectra of $\boldsymbol{k} \parallel \boldsymbol{c}$ configuration for undoped and Re-doped MoS_2 in figure 3 shows that excitons A and B for Re–MoS_2 are red shifted by 27 meV and 65 meV, respectively. The observed red shifts can be explained by the presence of rhenium impurity. A qualitative account of the rhenium-induced red shift can be understood as follows. During the formation of 3R-MoS_2, the rhenium ions can either substitute part of the Mo atoms in the MoS_2 lattice [14] or intercalate between the van der Waals gaps. From our previous study [31] it is most probable that the latter process predominated and resulted in the formation of 3R-MoS_2 in the doped sample. Consequently, the electronic states of the materials are perturbed together with the interlayer interactions. This effect results in the red shifting of the excitonic transitions with the energy separation of the spin orbit doublet reduced from 189 meV for undoped MoS_2 to 151 meV for Re–MoS_2. These values for energy separation agreed well with the literature [2, 20, 28, 31].

From figure 3, for Re–MoS_2, the spectra of $\boldsymbol{k} \parallel \boldsymbol{c}$ and $\boldsymbol{k} \perp \boldsymbol{c}$ configurations with $\boldsymbol{E} \perp \boldsymbol{c}$ polarization showed the measured difference for the peak positions of excitons A and B to be identical and equal to 21 meV. According to the earlier work by Liang [3], the two spectra obtained from $\boldsymbol{E} \perp \boldsymbol{c}$ should be similar since the wavevector of light is small compared with that of electrons and the spatial dispersion effects could be neglected. However, in this

work, appreciable deviation exists between the spectra of $\boldsymbol{E} \perp \boldsymbol{c}$ recorded from reflection off the van der Waals plane ($\boldsymbol{k} \parallel \boldsymbol{c}$) and edge plane ($\boldsymbol{k} \perp \boldsymbol{c}$) surfaces. The measured difference is being attributed to the crystal anisotropy [32, 33]. Our measurements should also offer better accuracy since previous experiments on MoS_2 always encounter the difficulty of inadequate working surface for recording reliable reflection spectra off the edge plane [3, 12]. In this work, such difficulty is not present due to the large edge plane surface available (2 mm × 10 mm). A qualitative account of crystal anisotropy can be understood as follows. The ground state excitonic transition in Re–MoS_2 can be described by a two-dimensional Mott–Wannier [29, 32, 34] hydrogen-like series $E_1 = E_g - R^*$, where E_g is the band gap and R^* is the effective Rydberg constant [32, 33] which is proportional to μ/ε^2. The parameter μ is the effective mass of the exciton and ε is the dielectric constant of MoS_2. The crystal anisotropy has been found to affect the dielectric constant perpendicular and parallel to the $\boldsymbol{c}$-axis with $\varepsilon_\perp > \varepsilon_\parallel$ for MoS_2 [20, 30]. The exciton effective mass is also determined to be affected by the crystal anisotropy with $\mu_\parallel > \mu_\perp$ [20, 26, 30]. As a result, we have $R^*_\parallel > R^*_\perp$. If we assume that E_g is not affected by the crystal anisotropy, we should have $E_{1_\perp} > E_{1_\parallel}$ for both excitons A and B. However, our experimental results indicate the opposite trend. Therefore it is reasonable to assume that crystal anisotropy also affect the band gap of the layered structure with $E_{g_\parallel} > E_{g_\perp}$. The band gaps of a number of layered transition metal dichalcogenides have been determined to be anisotropic along and normal to the crystal $\boldsymbol{c}$-axis with $E_{g_\parallel} > E_{g_\perp}$ [32, 35]. The crystal anisotropy induced red shift for the ground state is qualitatively given by $\Delta E = E_{1_\parallel} - E_{1_\perp} = E_{G_\parallel} - E_{g_\perp} + R^*_\perp - R^*_\parallel$. The measured crystal anisotropy induced red shift of 21 meV for Re–MoS_2 is about twice as large as those of WSe_2 by Chaparro *et al* [32].

For the spectra recorded from the edge plane surface ($\boldsymbol{k} \perp \boldsymbol{c}$) with $\boldsymbol{E} \perp \boldsymbol{c}$ and $\boldsymbol{E} \parallel \boldsymbol{c}$ polarization, the energies of exciton A are respectively at 1.833 eV and 1.838 eV resulting in a small red shift of 5 meV. The mechanism responsible for the detected difference may come from other origin. Exciton B is apparently unaffected by this mechanism. This is reasonable, as the linewidth of exciton B is much broader than exciton A. The measured shift of 5 meV though small is clearly present in the experimental spectra. A check on the reproducibility of the measured difference is undertaken by careful repetition of the experimentally recorded $\boldsymbol{E} \parallel \boldsymbol{c}$ and $\boldsymbol{E} \perp \boldsymbol{c}$ spectra and the result is consistent. An unpolarized spectrum is also recorded for comparison. We have found that the unpolarized spectrum can be obtained by taking an average of the two spectra with orthogonal polarization resulting in the 'average' peak position of exciton A at 1.836 eV. The physical origin of this shift can be realized qualitatively as follows. The intralayer bonding is part ionic and part covalent with the latter being dominant [12, 24]. The presence of Re atoms in the MoS_2 lattice has the effect of enhancing the ionicity of the metal–chalcogen bonding [36] as well as affecting the electronic states of the MoS_2 compound resulting in an increase of the lattice polarizability [12] of the Re–MoS_2. The lattice field interacting effect is much more pronounced for electric field perpendicular to the $\boldsymbol{c}$-axis than parallel to it [12]. This effect results in a shift of 5 meV in exciton A. The relatively weak effect is most likely due to the nature of the intralayer bonding of the MoS_2 lattice, which is predominantly covalent.

4. Summary

In summary, we have performed polarized EER measurements for both undoped and Re-doped MoS_2 samples. The presence of rhenium impurity has been determined to play a major role in influencing the measured differences in the recorded data. The Re ions intercalate between the van der Waals gaps of the 2H-MoS_2 lattice resulting in the formation of 3R-MoS_2. By comparing the spectra of $\boldsymbol{k} \parallel \boldsymbol{c}$ for undoped and Re-doped MoS_2 samples, the Re impurity

induced red shift for exciton A is determined to be 27 meV and for exciton B it is 65 meV. The crystal anisotropy induced red shifts for the doublets are identical and equal to 21 meV. Through a careful measurement of the $\boldsymbol{E} \perp \boldsymbol{c}$ and $\boldsymbol{E} \parallel \boldsymbol{c}$ polarizations EER spectra recorded off the edge plane surface of Re–MoS_2, the effect of the intralayer lattice field induced red shift of 5 meV (enhanced by the presence of Re) can be detected. The Re impurity is also observed to affect the symmetry selection rules of the excitonic transitions.

Acknowledgments

We would like to thank Professor Y S Huang of the Department of Electronic Engineering, National Taiwan University of Science and Technology, Taipei, Taiwan for many helpful discussions. We also want to thank Professor C H Ho of the Department of Electronic Engineering, Kuan Wu Institute of Technology and Commerce, Peitou, Taipei, Taiwan for helping with the crystal growth and technical assistance with the EER measurements. This work is supported by the National Science Council of the Republic of China under project number NSC 89-2112-M-019-002

References

[1] Wilson J A and Yoffe A D 1969 *Adv. Phys.* **18** 193
[2] Beal A R, Knights J C and Liang W Y 1972 *J. Phys. C: Solid State Phys.* **5** 3540
[3] Liang W Y 1973 *J. Phys. C: Solid State Phys.* **6** 551
[4] Tributsch H 1977 *Z. Naturf.* a **32** 972
[5] Kautek W, Gerisch H and Tributsch H 1980 *J. Electrochem.* **127** 2471
[6] Kam K K and Parkison B A 1982 *J. Phys. Chem.* **86** 463
[7] Bichsel R and Levy F 1985 *Thin Solid Films* **124** 75
[8] Li S J, Bernede J C, Ponzet J and Jamali M 1996 *J. Phys.: Condens. Matter* **8** 2292
[9] Martin J M, Donnet C and Mogne J L 1993 *Phys. Rev.* B **48** 10 583
[10] Yanagisama M 1993 *Wear* **168** 167
[11] Fleischaner P D 1987 *Thin Solid Films* **154** 309
[12] Weiser G 1973 *Surf. Sci.* **37** 175
[13] Clark A H 1970 *N. Jahrbuchf. Mineral. Monatsheffe* **3** 33
[14] Zelikman A N, Indenbaum G V, Teslitskaya M V and Shalankova V P 1970 *Sov. Phys.–Crystallogr.* **14** 687
[15] Tiong K K, Liao P C, Ho C H and Huang Y S 1999 *J. Cryst. Growth* **205** 543
[16] Cardona M, Shaklee K L and Pollak F H 1967 *Phys. Rev.* **154** 696
[17] Huang Y S and Cheng Y F 1988 *Phys. Rev.* B **38** 7997
[18] Aspnes D E 1980 *Optical Properties of Semiconductors (Handbook on Semiconductors)* ed M Balkanski (Amsterdam: North-Holland) p 109
[19] Pollak F H and Shen H 1993 *Mater. Sci. Eng.* R **10** 275
[20] Fortin E and Raga F 1975 *Phys. Rev.* B **11** 905
[21] Kasowski R V 1973 *Phys. Rev. Lett.* **30** 1175
[22] Bullet D W 1978 *J. Phys. C: Solid State Phys.* **11** 45 901
[23] Matteiss L F 1973 *Phys. Rev.* B **8** 3719
[24] Wood K and Pendry J B 1973 *Phys. Rev. Lett.* **31** 1400
[25] Coehoorn R, Haas C, Dijkstra J, Flispe C J F, de Groot R A and Wold A 1987 *Phys. Rev.* B **35** 6195
[26] Coehoorn R, Haas C and de Groot R A 1987 *Phys. Rev.* B **35** 6203
[27] Straub Th, Fauth K, Finteis Th, Hengsberger M, Claessen R, Steiner P, Hufner S and Blaha P 1996 *Phys. Rev.* B **53** 16 152
[28] Ho C H, Wu C S, Huang Y S, Liao P C and Tiong K K 1998 *J. Phys.: Condens. Matter* **10** 9317
[29] Beal A R and Liang W Y 1976 *J. Phys. C: Solid State Phys.* **9** 2459
[30] Bordas J and Davis E A 1973 *Phys. Status Solidi* b **60** 505
[31] Tiong K K, Shou T S and Ho C H *J. Phys.: Condens. Matter* at press
[32] Chaparro A M, Salvador P, Coll B and Gonzalez M 1993 *Surf. Sci.* **293** 881
[33] Yu P Y and Cardona M 1996 *Fundamentals of Semiconductors* (Berlin: Springer) p 266

[34] Chuang S L 1995 *Physics of Optoelectronic Devices* ed J W Goodman (New York: Wiley) p 102
[35] Ho C H, Huang Y S, Tiong K K and Liao P C 1998 *Phys. Rev.* B **58** 16 130
[36] Beal A R and Hughes H P 1979 *J. Phys. C: Solid State Phys.* **12** 881